Molecular Crystals and Liquid Crystals Science and Technology. Section A. Molecular Crystals and Liquid Crystals

Publication details, including instructions for authors and subscription information:
http://www.tandfonline.com/loi/gmcl19

^{1}H-Overhauser Shift in Radical Cation Salts

B. Gotschy [a] & G. Denninger [a]

[a] Physikalisches Institut and Bayreuther Institut für Makromolekülforschung, Universität Bayreuth, Postfach 101251, D-8580, Bayreuth, Federal Republic of Germany

Version of record first published: 24 Sep 2006.

To cite this article: B. Gotschy & G. Denninger (1993): ^{1}H-Overhauser Shift in Radical Cation Salts, Molecular Crystals and Liquid Crystals Science and Technology. Section A. Molecular Crystals and Liquid Crystals, 237:1, 435-444

To link to this article: http://dx.doi.org/10.1080/10587259308030155

Mol. Cryst. Liq. Cryst., 1993, Vol. 237, pp. 435–444
Reprints available directly from the publisher
Photocopying permitted by license only

Printed in the United States of America

^{1}H-Overhauser Shift in Radical Cation Salts

B. GOTSCHY and G. DENNINGER

Physikalisches Institut and Bayreuther Institut für Makromolekülforschung, Universität Bayreuth, Postfach 101251, D-8580 Bayreuth, Federal Republic of Germany

(Received October 15, 1991; in final form November 16, 1992)

Radical cation salts of planar aromatic pure hydrocarbons are model systems for quasi-one-dimensional organic conductors. The mobility of the conduction electrons leads to a strong motional narrowing of the electron spin resonance (ESR). These narrow lines allow detailed investigations of the Overhauser shift of the ESR. This shift is caused by hyperfine interaction of the conduction electrons with protons and ^{13}C. By a double resonance technique this shift can be measured, and investigations of NMR saturation and nuclear relaxation times are presented. The lineshape of the ^{1}H-resonance is dominated by dipolar proton-proton coupling. We show that the Overhauser shift technique is similar to common CW-NMR but with an improved sensitivity.

Keywords: radical cation salts, Overhauser shift, dynamic nuclear polarization

1. INTRODUCTION

Organic radicals in solution usually exhibit a resolved hyperfine structure in their ESR spectrum due to the hyperfine interaction of the radical electron spin with the magnetic moments of the nuclei. Each magnetically nonequivalent nucleus contributes to the spectrum. In solids often another situation prevails. The interaction of the electron spins with the electrons on neighbouring molecules causes a broadening of the ESR transition and the hyperfine components finally overlap. One finds only a single ESR line which is inhomogeneously broadened. Considering only dipolar coupling between two electron spins on adjacent molecules in radical cation salts about 3.5 Å apart yields an ESR line width of about 200 MHz. In organic radical ion salts the observed line widths are several orders of magnitude smaller.

The statements made so far are only valid, if the correlation time τ_c of the electron spin on a molecule is long compared to the timescale of the Larmor precession. This condition is no longer valid in the radical cation salts. These systems possess a metallic high temperature phase (see Section 2) with $\tau_c = \hbar/E_F \sim 10^{-15}$ s, an order of magnitude which is characteristic for many metals. Under these conditions an electron spin interacts with many nuclei with different nuclear spin orientations and the hyperfine interaction is nearly completely averaged out. Due to the nonzero polarization $\langle I_z \rangle$ of the nuclei in the static field B_0 only the ensemble average A_{zz} of the hyperfine interaction in the direction of B_0 remains (B_0 is taken along the

z-axis). Now the ESR spectrum consists of a strongly motional narrowed single ESR line, which is shifted in field by an amount ΔB_{ov} with $\Delta B_{ov} \propto A_{zz} \cdot \langle I_z \rangle$ compared to the resonance field of noninteracting electron spins. This shift is denoted as Overhauser shift. As will be shown, this shift is of the order of some mG for protons at room temperature, and because the ESR line width in the radical cation salts is also in the same range, it can be easily detected.

Meanwhile a lot of experiments were done on this topic (for a review the reader is referred to Reference 1 and the references cited therein). The aim of this article is to discuss especially the Overhauser shift of the protons in radical cation salts.

2. RADICAL CATION SALTS

Radical cation salts are model systems for one type of organic conductors. Here the cations are oxidized (electron charge +1, electron spin $S = 1/2$) planar aromatic hydrocarbons with an extended π-electron system, the so-called arenes. The counterions are usually centrosymmetric such as PF_6^- or AsF_6^-.

A characteristic feature of these systems is the arrangement of the molecules in stacks. The organic stacks are well separated from the counterions, which occupy the positions between the stacks. This arrangement leads to a high degree of one-dimensionality in the properties of these salts, for example a high anisotropy of the conductivity[2,3] (high conductivity along the stacks, low conductivity perpendicular to the stacks).

Due to a dimerisation of the organic molecules, a charge transfer of one electron per dimer to the counterions and the favourable close spacing along the stacking direction the radical cation salts show metallic-like conducting behaviour above a critical temperature T_c (high temperature phase). At lower temperatures the radical cation salts undergo a phase transition and become semiconducting. In this article we will concentrate on measurements in the high temperature phase.

We investigated radical cations salts of fluoranthene,[4] in the following abbreviated as FA, pyrene[4] and perylene.[5] Figure 1 gives a crude sketch of the systems under consideration. The crystallographic axis denoted in Figure 1 as *a* is the axis of the highest conductivity. The molecules are stacked along *a*. The crystals are usually growing along *a*, giving rise to a needle-like shape. For further information the reader is referred to the References. Only a few details, which seem to be specific to our salts, which were all grown electrochemically in our crystal-growing laboratory at Bayreuth, shall be mentioned.

1. $FA_2^+ PF_6^-$: The ESR line width of less than 20 mG is extremely narrow for the solid state. Meanwhile stable crystals with a weight of a few mg and good quality can be grown.[6]
2. Pyrene is forming radical cation salts in the presence of appropriate counter ions, and single crystals can be grown. But in contrast to $FA_2^+ PF_6^-$ various stoichiometries are reported.[4] However, the results presented here can be interpreted as molecular properties and the exact composition is of minor importance to our results. Thus, for convenience the notation $(\text{pyrene})_2^+ \cdot PF_6^-$ will be used further. But we want to emphasize, that we do not know

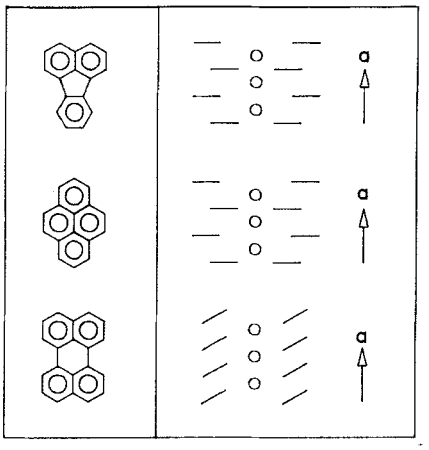

FIGURE 1 Schematic sketch of the systems under consideration. Left: molecular structure, right: crystal structure. The stacking axis *a* is indicated. Top: FA_2PF_6, middle: $pyrene_2PF_6$, bottom: $perylene_2PF_6$.

exactly the composition of our salts. The ESR line width is between 40 and 50 mG, slightly sample dependent.

3. The 2:1 stoichiometry of perylene radical cation salts seems to be undisputed, but a variety of crystal structures were reported.[7] Some of these structures seem to be metastable. We found two types of perylene salts. The first, denoted as $(perylene)_2^+ PF_6^-$ (I), showed an ESR line width of 40 mG. The second, denoted as $(perylene)_2^+ PF_6^-$ (II), showed an ESR line width of 500 mG. By careful tempering (100°C for 60 min) the line width could be reduced to 70–150 mG in the latter one. This clear decrease of the line width indicates a better mobility of the electrons. Either the packing and thus the molecular overlap along the stacks is improved or the thermal treatment causes included solvents to split off. Anyhow, the reduction of the line width is accompanied by the appearance of a 2 G broad line. This line is probably caused by fixed paramagnetic impurities, similar to FA_2PF_6.[8] But so far no relation between reported crystal structures and our two perylene systems could be made.

3. EXPERIMENTAL SETUP

The basic Overhauser shift experiment reduces the nuclear spin polarization $\langle I_z \rangle$ to zero by application of a saturating radiofrequency field (RF) at the NMR frequency of the respective nucleus,[9] whereby the Overhauser shift ΔB_{ov} is canceled. For this purpose, a double resonance cavity (standard *X*-band ENDOR resonator, Bruker, ESR frequency 9.42 GHz) is used and the NMR frequency is swept over the appropriate region. Beside these CW-NMR experiments we have also done time resolved measurements. After saturation of the NMR the RF is switched off and the temporal evolution of the Overhauser shift, which is equivalent to the time dependence of $\langle I_z \rangle$, is observed. Thereby the longitudinal nuclear relaxation time T_1 can be extracted.

We used our "triple lock," an improved version of the "Overhauser Lock"[10] for field frequency stabilization. Details of the setup will be published elsewhere.

A temperature range of 4.2–300 K was accessible. All crystals were oriented with the needle axis parallel to the static field B_0. This axis is the one which can be identified unambiguously and we will restrict the discussion to measurements in this orientation.

4. ^{1}H-OVERHAUSER SHIFT

The spin Hamiltonian H of an electron with spin **S** interacting with a nuclear spin **I** through hyperfine coupling A is given by

$$H = g^* \cdot \mu_B \cdot B_0 \cdot S_z + \mathbf{I} \cdot \underline{\mathbf{A}} \cdot \mathbf{S}$$

where B_0 is the static field along z, μ_B the Bohr magneton and g^* the effective g-factor of the electron. $\underline{\mathbf{A}}$ is the hyperfine tensor, which is the sum of the isotropic Fermi-type coupling and the anisotropic dipolar part. In organic systems g^* is close to the value g_0 of free electrons, indicating a small spin orbit coupling. For conduction electrons in metals and semiconductors the correlation time τ_c of an electron spin at a nuclear position is of the order of 10^{-15} s. In this case, only an averaged hyperfine interaction is observed. The effective electron spin Hamiltonian H_e is

$$H_e = g^* \cdot \mu_B \cdot B_0 \cdot S_z + A_{zz} \cdot \langle I_z \rangle \cdot S_z = g^* \cdot \mu_B \cdot (B_0 + \Delta B_{ov}) \cdot S_z$$

$\langle I_z \rangle$ is the ensemble average of I_z over all equivalent lattice nuclei, A_{zz} is the tensor component parallel to B_0 and ΔB_{ov} is the nuclear field. Only one nuclear species is considered; the extension to several nuclei is straightforward. Due to the nonzero polarization $\langle I_z \rangle$ of the nuclei in the static field B_0 the hyperfine interaction is not completely averaged out, but a residue remains. Its longitudinal component shifts the electron spin resonance by an amount $\Delta B_{ov} = A_{zz} \cdot \langle I_z \rangle / (g^* \cdot \mu_B)$. This is the Overhauser shift.

For a proton in a C—H bond of an aromatic radical A_{zz} is caused by a pseudoscalar hyperfine interaction. According to the McConnell relation[11] we can write $A_{zz} = -65$ MHz $\cdot \rho$ where ρ is the π-spin density on the carbon atom in the bond and we get $\Delta B_{ov} \propto \rho$. Thus a measurement of ΔB_{ov} provides a direct determination of ρ. This relation is the most important aspect of the Overhauser shift technique, since magnetic nuclei can be used as "local probes" for the conduction electron wave function.

By sweeping a saturating RF field through the nuclear resonance position one observes a shift of the ESR due to the reduction of $\langle I_z \rangle$ by saturation. This shift is recorded. An absolute calibration can be done by a simple gauge measurement, and one can finally extract ΔB_{ov}. However, we want to emphasize, that we observe no NMR spectrum in the usual sense. The spectra to be shown here are rather hyperfine interaction versus frequency than intensity versus frequency.

The enhancement of the nuclear spin polarization by saturation of the CESR

has been predicted in metals by Overhauser[12] and has been observed in metals,[13] semiconductors[14,15,16] and organic conductors.[9] A theoretical analysis was given by Solomon.[17] The dependence of the nuclear spin polarization $\langle I_z \rangle$ on the CESR saturation parameter s is given by $\langle I_z \rangle = \langle I_0 \rangle \cdot (1 + V \cdot s)$. $\langle I_0 \rangle$ is the nuclear spin polarization in thermal equilibrium and $s = (\langle S_0 \rangle - \langle S_z \rangle)/\langle S_0 \rangle$, with $0 < s < 1$.

V is the Overhauser enhancement factor, which depends on the details of the hyperfine interaction and the nuclear relaxation mechanisms. For protons V can vary between -658 for pure dipolar and $+658$ for pure scalar hyperfine interaction. For a detailed discussion of V see Reference 1. Thus by partial saturation of the CESR large dynamic nuclear polarization effects are expected and the Overhauser shift increases proportional to $\langle I_z \rangle$. The detection of the Overhauser shift provides a very sensitive method for measurements in the nuclear system by detecting the NMR via the ESR. For example nuclear T_1 measurements can be made in very small single crystals of radical cation salts (sample weight about 1 μg), where usual NMR methods fail.

As already mentioned the principle of our experiments is to measure the nuclear hyperfine field, which is proportional to $\langle I_z \rangle$, by sweeping the RF over the NMR of the nucleus under consideration. In these CW experiments the frequency dependence of $\langle I_z \rangle$ can be described by the Bloch equations.[18] This yields finally:

$$\Delta B_{ov} = \frac{\Delta B_{ov}^{\max}}{1 + (\omega - \omega_0)^2/\Delta\omega^2 + \omega_1^2 \cdot T_1/\Delta\omega}$$

T_1 is the nuclear spin lattice relaxation time, ω_1 is the amplitude and ω the frequency of the RF field and $\Delta\omega$ the half width at half height of the nuclear transition at ω_0. Exactly at resonance ($\omega = \omega_0$) and using the RF power P instead of ω_1^2 we get:

$$\Delta B_{ov}(P) = \Delta B_{ov}^{\max} \cdot \frac{1}{1 + b \cdot P \cdot T_1} \tag{1}$$

with a parameter b. $\Delta B_{ov}^{\max}$ is the Overhauser shift without saturation of the NMR. Before proceeding with details of the method we want to say a few words about the overall procedure. Measurements were performed at various power levels. At a relatively low power level the signal is independent of the RF power. The signal amplitude goes to zero for vanishing RF power. The NMR is unsaturated. The ESR is found at $B_0 + \Delta B_{ov} \cdot (1 + V \cdot s)$. Above saturation ($b \cdot P \cdot T_1 \simeq 1$) the line width increases. This phenomenon is known as saturation broadening.[19] Far above saturation the NMR is completely saturated ($\langle I_z \rangle = 0$). The ESR is found at B_0 and ΔB_{ov} is zero. This should not be confused with saturation in classical CW-NMR where the intensity of absorption also goes to zero. However, one would expect a maximum for the intensity at $b \cdot P \cdot T_1 \simeq 1$, whereas in our case ΔB_{ov} goes continuously to zero. We made power dependent measurements of the ^{1}H-Overhauser shift in the four radical cation salts mentioned before. ΔB_{ov} varies between about 20 μG ($P \rightarrow \infty$) and 5 mG ($P \rightarrow 0$). The value of 5 mG indicates, that isotropic hyperfine interaction is the dominant coupling mechanism, since at 200 K the largest possible shift is 13.5 mG for complete ESR saturation and for $V =$

658. Typical ESR saturation levels are $s \simeq 0.7$. Thus V is typical 350 ($a \parallel B_0$) for our four radical cation salts in agreement with earlier measurements in FA_2PF_6.[9] The results are shown in Figure 2 together with a fit to Equation (1). All data in Figure 2 are scaled to unity, that means $\Delta B_{ov} = 0$ for high power and $\Delta B_{ov} = 1$ for low power. T_1 can be measured separately. The only parameter of the fit is b ($\omega_0 = 90 \cdot 10^6\ s^{-1}$, $T = 200$ K). b is proportional to the transversal relaxation time $T_{2,eff}$,[19] which determines the homogeneous NMR line width $\Delta\omega$ (i.e. for a Lorentzian lineshape one has $\Delta\omega = 2 \cdot T_{2,eff}^{-1}$. $\Delta\omega$: FWHM). We write $T_{2,eff}$ instead of T_2 to indicate that it is the average of all protons on the molecule. To calculate $T_{2,eff}$ from b, one has to calibrate the NMR coil. We found for the dependence between RF power P and ω_1: $\omega_1 = 13.5 \cdot 10^3\ s^{-1} \cdot P^{1/2}$. So $T_{2,eff}$ can be extracted from b and the values found here are compiled in Table I together with our values of T_1. It is interesting to note, that T_1 in perylene(II) is not influenced by the higher defect concentration compared to perylene(I). Hyperfine interaction with the conduction electrons is the dominant source of nuclear relaxation. This is further indicated by the high V values. DNP is strongly depressed if other relaxation mechanisms become important.[1]

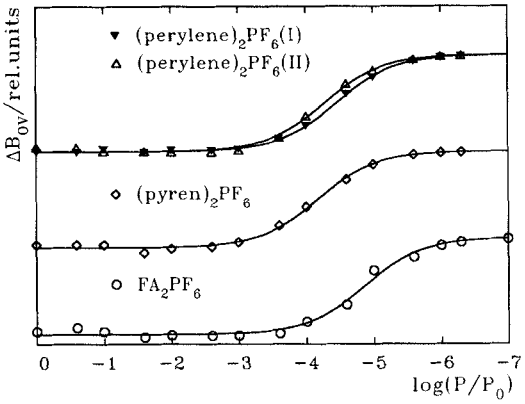

FIGURE 2 ^{1}H-Overhauser shift versus RF power together with a fit to equation 1. $P_0 = 100$ W, $T = 200$ K.

TABLE I

T_1 was measured. $T_{2,eff}$ was determined from the fit in Figure 2. The experimental error is about 10% for all values ($T = 200$ K)

	T_1/ms	$T_{2,eff}$/ms
FA_2PF_6	420	1.29
pyrene$_2$PF$_6$	80	1.39
perylene$_2$PF$_6$(I)	170	1.25
perylene$_2$PF$_6$(II)	170	0.83

5. ^{1}H-LINESHAPE

$\Delta\omega$ or $T_{2,\text{eff}}$ is characteristic for the width of the NMR line of an isolated proton, which would be of the order of 1 kHz. Of course in these molecules we do not have isolated proton spins. The protons feel the dipolar coupling to neighboring protons. At saturating RF powers the ^{1}H line has a Lorentzian shape and the line width increases proportional to $\sqrt{P}$.[19] A lowering of the RF power causes appreciable deviations from the Lorentzian shape. Two shoulders appear (Figure 3), which are caused by dipolar proton-proton interaction. In deuterated samples (proton contents <5%) the protons are magnetically diluted and proton-proton interaction can be neglected. Hence the shoulders are missing (Figure 3). However, so far, deuterated samples always suffer from a poorer sample quality. Broader ESR lines prevail, which makes the detection of small Overhauser shifts much harder. Furthermore $\Delta B_{ov}^{\max}$ scales with the proton content and thus the signal to noise ratio is strongly decreased. Therefore we had to use stronger RF fields to detect the ^{1}H-shift in the deuterated sample (for technical reasons, which will not be discussed in this paper, our signal is maximum for complete and zero for vanishing saturation; a gauge measurement yields the real ΔB_{ov}). A partial saturation broadening prevails. The lineshape shall now be discussed in non-deuterated samples. The analysis will be explained in details for FA_2PF_6 where a precise crystal structure[4] and local resolved spin densities are available.[20] We will further concentrate on $a \parallel B_0$, which simplifies the discussion. For $a \parallel B_0$ all C—H bonds are perpendicular to the static field. Our calculations will follow the theory developed in the paper of Andrew and Bersohn.[21]

Figure 4 shows that the main contributions to the dipolar interaction of a given proton are due to the coupling to two neighbouring protons. For example, for position 4 it is the dipolar coupling with positions 3 and 5. The coupling to all other protons, which decreases with the cube of the distance, will be disregarded in first order. For example, the coupling between 4 and 8 is more than one order of

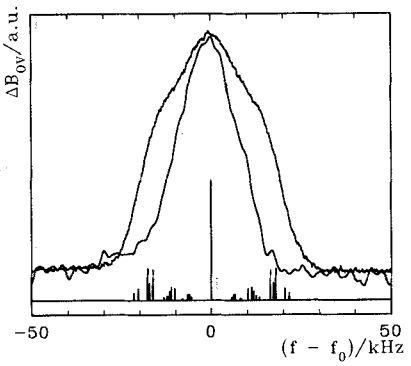

FIGURE 3 Broad line, ^{1}H-Overhauser shift in FA_2PF_6 at very low RF power. Two shoulder, about 34 kHz apart are visible. Narrow line, ^{1}H-Overhauser shift in partially deuterated FA_2PF_6. Proton contents about 5%. The protons can be regarded as magnetically dilute. For a better comparison of the lineshape both spectra are plotted with the same amplitude. Bottom, calculated intensity profile, for details see text. To distinguish it from the measured spectra the base line is shifted.

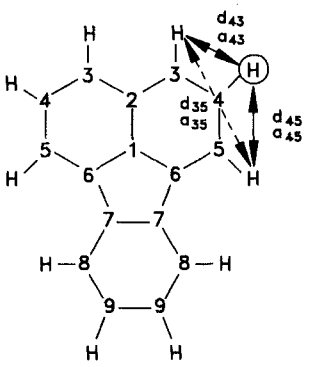

FIGURE 4 FA molecule. For a proton in position 4 the dipolar coupling (a_{ij}) to the next two neighbours (distance d_{ij}) is indicated. (d_{43} = 2.32 Å, a_{43} = 9.53 kHz, d_{45} = 2.39 Å, a_{45} = 8.72 kHz, d_{35} = 4.08 Å, a_{35} = 1.75 kHz).

magnitude smaller than the coupling between 3 and 4 or 4 and 5. So, the problem of calculating the NMR spectrum for FA_2PF_6 can be separated into several subproblems, where one has to consider only the dipolar coupling for a triangular configuration of protons (3–4–5, 4–5–8 and so on). The distance to protons on neighbouring molecules is much larger than intramolecular proton-proton distances. Thus the NMR spectrum turns out to be a molecular property, at least for FA_2PF_6. For each configuration we get 7 resonance positions with the respective transition probabilities. Now we must remember that we measure always rather hyperfine interaction than pure transition probabilities. The hyperfine interaction for a proton is proportional to the π-spin density, which was taken from Reference 20. Finally we multiplied the transition probabilities with the respective hyperfine interaction. Figure 3 (bottom) shows the calculated resonance positions for a FA molecule together with the corresponding intensity profile.

One can see a group of 3 lines on each side of the central peak with increased intensity. These two groups are separated by about 34 kHz, which corresponds roughly to the spacing of the two shoulders of the ^1H line in Figure 3. Thus we get a crude idea of the ^1H-lineshape. However, if we interpret $T_{2,\text{eff}}$ as a residual broadening of each transition of about 0.3 kHz we should see much more structure in our spectra. Obviously our analysis is still insufficient or other sources of broadening are important. However, we can conclude, that the origin of the lineshape is due to intramolecular proton-proton interactions. All the other protons will be reflected in the second moment.

The ^1H line of pyrene$_2PF_6$ is nearly identical to that of FA_2PF_6 because the similar molecular geometries give rise to similar proton-proton distances. The lineshape indicates the dominance of intramolecular proton couplings. It is thus not worthwhile to present details of the pyrene line. But we want to emphasize that the lineshape is here again a molecular problem and the real stoichiometry is of minor importance.

The situation becomes more complicated for perylene$_2PF_6$. All crystal structures reported[7] show that for some positions on the perylene molecule intermolecular proton-proton distances are comparable to intramolecular distances. Thus the sim-

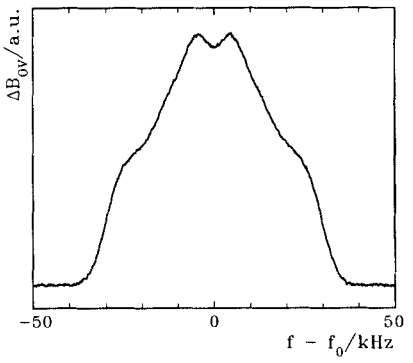

FIGURE 5 ^{1}H-Overhauser shift in (perylene)$_2PF_6$ at very low RF-power.

ple model of above fails. The lineshape (Figure 5) has much more structure than in the case of pyrene$_2PF_6$ or FA_2PF_6. Without a crystal structure for our salts it seems to be impossible to make a lineshape analysis which goes beyond a pure qualitative interpretation.

One final point shall be mentioned: As one raises the RF power the line begins to broaden and the structure in Figure 3 or Figure 5 is smeared out. So one is forced to work with very low RF powers, far below saturation. On the other hand ESR saturation does not influence the NMR besides an enhancement of the nuclear polarisation, which increases the signal amplitude. Thus, we always worked with high microwave powers.

Our calculations of the lineshape is based on a triangular configuration of protons. Thereby we have to calculate three coupling constants. One of them is always much smaller than the other two. So one must ask, if such a rigorous treatment is really necessary. We also tried simulations of the lineshape, where we only included pairwise interactions of each proton with its two neighbouring protons. For such a proton pair one gets immediately the expectation values of the nuclear spin, and the secular term and the flip flop term of the dipol operator can be calculated easily. We used such a simple model for an analysis of the lineshape of ^{13}C-Overhauser shifts. There the lineshape is dominated by the dipolar coupling of a carbon to the proton in the C—H bond. The coupling to all other protons is much smaller and one has to calculate only one coupling for each carbon. Details can be found elsewhere.[22] For qualitative calculations it seems to be justified to consider only pairwise interaction.

6. CONCLUSION

Progress in the material sciences led to the preparation of systems with very interesting magnetic properties. The development of new magnetic resonance techniques like measurements of the Overhauser shift was triggered by the availability of single crystals of organic conductors with rather narrow ESR lines. With this new double resonance technique we have investigated the ^{1}H-Overhauser shift in

single crystals of the radical cation salts of fluoranthene, pyrene and perylene. In this paper we show the results of the power dependence of the ^{1}H-Overhauser shift. Thereby we presented a new access to the determination of the transverse nuclear relaxation time T_2. Measurements of the longitudinal nuclear relaxation time T_1 via the Overhauser shift were already published.[9] Thus, one of the advantages of the Overhauser shift technique is, that it allows the study of nuclear relaxation even in small single crystals where usual NMR methods fail. The possibility to polarize the nuclei dynamically can enhance the sensitivity by more than two orders of magnitude compared to common NMR. Furthermore we studied the lineshape of the ^{1}H resonance line. It was shown, that this can be explained by dipolar proton-proton coupling, whereby for a description of the lineshape the molecular structure and the π-spin densities on each carbon position in the molecula are necessary. Vice versa the lineshape can be used to determine the spin densities and to make qualitative proposals of the crystal structure.[22] All together the Overhauser shift technique turned out to be a valuable tool for analysing the properties of the nuclear system because of its high sensitivity. Furthermore, it offers the possibility to use the nuclei as microprobes for the wave function of the electrons.

Acknowledgment

We like to thank M. Schwoerer and E. Dormann for stimulating and critical discussions. This work was supported by Stiftung Volkswagenwerk and DFG (SFB 213).

References

1. G. Denninger, *Mol. Cryst. Liq. Cryst.*, **171**, 315 (1989).
2. T. Schimmel, W. Rieß, J. Gmeiner, G. Denninger and M. Schwoerer, *Solid State Comm.*, **65**, 1311 (1988).
3. W. Stöcklein, B. Bail, M. Schwoerer, D. Singel and J. Schmidt, "Organic Molecular Aggregates," eds. P. Reineker, H. Haken and H. C. Wolf, Springer Series in Solid State Science, 49 (1983).
4. V. Enkelmann, B. S. Morra, C. Kröhnke, G. Wegner and J. Heinze, *Chem. Phys.*, **66**, 303 (1982).
5. P. Koch, D. Schweitzer, R. H. Harms, H. J. Keller, H. Schäfer, H. W. Helberg, R. Wilckens, H. P. Geserich and W. Ruppel, *Mol. Cryst. Liq. Cryst.*, **86**, 87 (1982).
6. U. Köbler, J. Gmeiner and E. Dormann, *J. Magn. Magn. Mat.*, **69**, 189 (1989).
7. H. Endres, H. J. Keller, B. Müller and D. Schweitzer, *Acta Cryst.*, **C41**, 607 (1985).
8. E. Dormann and G. Sachs, *Ber. Bunsenges. Phys. Chem.*, **91**, 879 (1987).
9. W. Stöcklein and G. Denninger, *Mol. Cryst. Liq. Cryst.*, **136**, 335 (1986).
10. G. Denninger, *Bruker Report*, **1**, 18 (1987).
11. H. M. McConnell and D. B. Chesnut, *J. Chem. Phys.*, **28**, 107 (1958).
12. A. W. Overhauser, *Phys. Rev.*, **92**, 411 (1953).
13. Ch. Ryter, *Phys. Rev.*, **5**, 10 (1960).
14. B. Gotschy, G. Denninger, H. Obloh, W. Wilkening and J. Schneider, *Solid State Comm.*, **71**, 629 (1989).
15. B. Clerjaud, F. Gendron, H. Obloh, J. Schneider and W. Wilkening, *Phys. Rev.*, **B40**, 404 (1989).
16. G. Denninger and H. Pascher, *Solid State Comm.*, **70**, 399 (1989).
17. I. Solomon, *Phys. Rev.*, **99**, 559 (1955).
18. F. Bloch, *Phys. Rev.*, **70**, 463 (1946).
19. A. Abragam, "The Principles of Nuclear Magnetism," Oxford, Clarendon Press, 104 (1973).
20. D. Köngeter and M. Mehring, *Phys. Rev.*, **B39**, 6361 (1989).
21. E. Andrew and R. Bersohn, *J. Chem. Phys.*, **18**, 159 (1950).
22. B. Gotschy and G. Denninger, *Molec. Phys.*, **69**, 169 (1990).